

A Ground Motion Prediction Equation for the Horizontal Component of Cumulative Absolute Velocity (CAV) Based on the PEER-NGA Strong Motion Database

Kenneth W. Campbell,^{a)} M.EERI, and Yousef Bozorgnia,^{b)} M.EERI

Cumulative absolute velocity (CAV), defined as the integral of the absolute acceleration time series, has been used as an index to indicate the possible onset of structural damage to nuclear power plant facilities and liquefaction of saturated soils. However, there are very few available ground motion prediction equations for this intensity measure. In this study, we developed a new empirical prediction equation for the horizontal component of CAV using the strong motion database and functional forms that were used to develop similar prediction equations for peak response parameters as part of the PEER Next Generation Attenuation (NGA) Project. We consider this relationship to be valid for magnitudes ranging from 5.0 up to 7.5–8.5 (depending on fault mechanism) and distances ranging from 0–200 km. We found the interevent, intra-event, and intracomponent standard deviations from this relationship to be smaller than any intensity measure we have investigated thus far. [DOI: 10.1193/1.3457158]

INTRODUCTION

Cumulative absolute velocity (CAV), which is defined as the integral of the absolute value of the acceleration time series, is represented mathematically by the equation (EPRI 1988):

$$\text{CAV} = \int_0^{t_{\max}} |a(t)| dt \quad (1)$$

where $|a(t)|$ is the absolute value of the acceleration time series at time t and t_{\max} is the total duration of the time series. Figure 1 shows a hypothetical acceleration time series and the corresponding value of CAV as it evolves over time. In this figure, CAV is the summation of the shaded areas. It is evident from the definition of CAV that its value increases with time until it reaches its maximum value at t_{\max} . Therefore, CAV includes the cumulative effects of ground motion duration. This is a key advantage of CAV over peak response parameters and is one of the reasons that EPRI (1988) found it to be the instrumental intensity measure that best correlated with the onset of structural damage to engineered structures. However, it

^{a)} EQECAT, Inc., 1030 NW 161st Place, Beaverton, OR 97006-6337

^{b)} Pacific Earthquake Eng. Research Center, 325 Davis Hall, University of California, Berkeley, CA 94720-1792

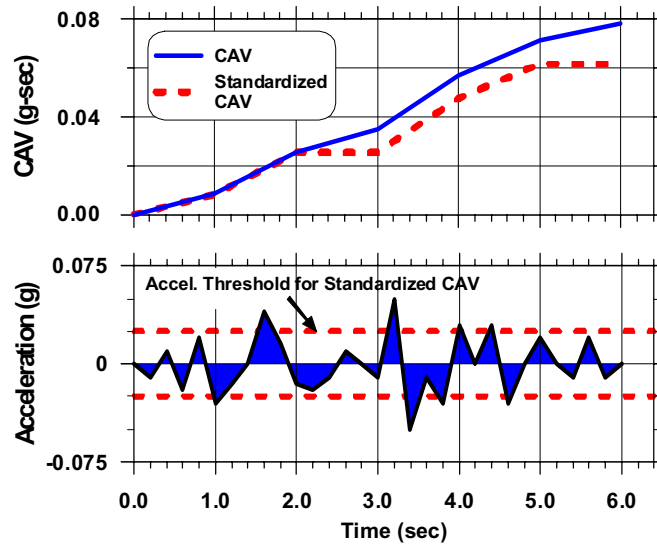


Figure 1. Illustration of the definition of CAV showing its evolution with time (modified from EPRI 1988).

should be noted that CAV does not account for the timing of the arrival of the different phases of energy such as a large velocity pulse.

Although named the cumulative absolute velocity, CAV is not directly related to the ground motion velocity, $v(t)$, although it does have units of velocity. The name cumulative absolute velocity comes from the recognition that, since $v(t) = \int a(t) dt$, the integral over acceleration in Equation 1 can be rewritten as the following summation of incremental (i.e., peak-to-valley and valley-to-peak) velocities, regardless of sign, in the velocity time series (EPRI 1988):

$$CAV = \sum_{i=1}^N |\Delta v_i| \quad (2)$$

where Δv_i is the i th value of incremental velocity in the time series and N is the total number of incremental velocities.

CAV was initially developed and proposed by EPRI (1988) as an index to indicate the onset of structural damage to engineered structures. Since then several variants of CAV have been proposed that are believed to be better suited to specific engineering applications. EPRI (1991) proposed a standardized version of CAV, denoted herein as CAV_{STD} , that excluded any nonoverlapping one-second interval of a recording, inclusive of the endpoints, in which the peak acceleration was less than 0.025 g (Figure 1). In this way, non-damaging portions of long, small-amplitude acceleration records were prevented from contributing to CAV. The U.S. Nuclear Regulatory Commission (USNRC 1997) subse-

quently adopted CAV_{STD} as the ground motion intensity measure used to determine whether a nuclear power plant must be shut down if the Operating Basis Earthquake (OBE) response spectrum is exceeded in an earthquake. [EPRI \(2006\)](#) developed a ground motion prediction equation (GMPE) for CAV_{STD} using the Pacific Earthquake Engineering Research Center Next Generation Attenuation (PEER-NGA) strong motion database and, together with [Watson-Lamprey and Abrahamson \(2007\)](#), proposed the use of a minimum value of CAV_{STD} to exclude small magnitude (non-damaging) earthquakes from contributing to a probabilistic seismic hazard analysis (PSHA). [Kramer and Mitchell \(2006\)](#) found that a version of CAV that excludes those acceleration pulses with accelerations less than 5 cm/sec^2 (0.005 g) was the best intensity measure to relate to the generation of excess porewater pressure in potentially liquefiable soils. They refer to this CAV intensity measure as CAV_5 and demonstrated its predictability by developing a GMPE using a subset of the PEER-NGA database.

CAV has been shown to correlate indirectly with damage through its strong relationship with other proposed damage indices. [Cabañas et al. \(1997\)](#) found a strong relationship between a modified version of CAV_{STD} , with a cutoff of 20 cm/sec^2 ($\sim 0.02 \text{ g}$) instead of 0.025 g , with both the local macroseismic intensity and the damage level of structures observed during four earthquakes in Italy. [Koliopoulos et al. \(1998\)](#) developed relationships between CAV, local macroseismic intensity, and Housner Intensity ([Housner 1959](#)) using recordings from the Greek strong motion database and found a strong correlation with Housner Intensity (coefficient of determination of $R^2=0.78$). [Kostov \(2005\)](#) used several strong motion databases in Europe to correlate CAV_{STD} with macroseismic intensity, magnitude, and distance and concluded that it was a better predictor than PGA of the expected damage from scenario earthquakes at a nuclear power plant in Bulgaria. [Klügel et al. \(2006\)](#) suggested that CAV could be used to define the ductile (low cycle fatigue) failure mode condition of structures and components and recommended that it be used to scale ground motions for scenario earthquakes used in ductile design. [Danciu and Tselentis \(2007\)](#) used recordings from the Greek strong motion database to develop a GMPE for CAV and found that it had the smallest standard deviation of any of the peak response and energy related intensity measures that they evaluated, including PGV, Arias Intensity ([Arias 1970](#)), Housner Intensity, and root-mean-square acceleration. [Martinez-Rueda et al. \(2008\)](#) correlated CAV with Housner Intensity using the European strong motion database and found a strong correlation ($R^2=0.81$) between these two intensity measures. [Tselentis and Danciu \(2008\)](#) developed relationships between local macroseismic intensity and CAV from earthquakes in Greece and found that the correlation, as measured by the standard deviation (they did not report R^2), was greatly improved by including magnitude, distance, and site conditions in the relationship.

Although CAV has not yet been used in any engineering applications as CAV_{STD} and CAV_5 have, [Campbell and Bozorgnia \(2010\)](#) showed that, compared to these other versions, CAV is relatively stable and predictable. The decrease in stability of CAV_{STD} and CAV_5 is caused by the relatively large number of zero values and the rapid decrease in values near the acceleration threshold. This makes CAV suitable for use in developing a base GMPE from

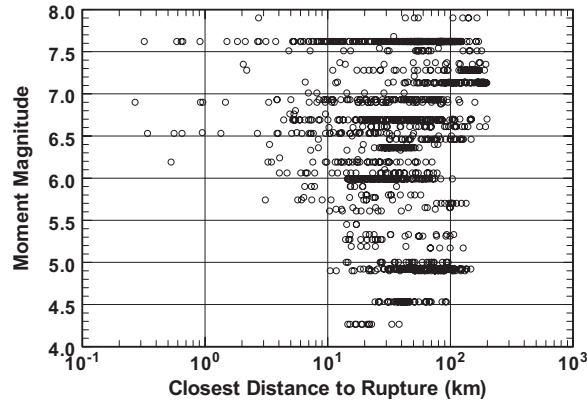


Figure 2. Distribution of recordings with respect to moment magnitude (M) and rupture distance (R_{RUP}).

which reliable estimates of CAV_{STD} and CAV_5 can be derived (e.g., [Campbell and Bozorgnia 2010](#)). Alternatively, [Stafford \(2008\)](#) has proposed a random-effects method that can be used to account for these zero values.

The GMPE for CAV developed in this paper builds on a four-year multidisciplinary study that was sponsored by PEER to develop Next Generation Attenuation (NGA) relationships for shallow crustal earthquakes in active tectonic regions ([Power et al. 2008](#)). This study is currently referred to as the NGA-West Project. The new CAV relationship complements our existing NGA-West relationships for peak ground acceleration (PGA), peak ground velocity (PGV), peak ground displacement (PGD), 5%-damped linear-elastic response-spectral acceleration (PSA), and inelastic response-spectral acceleration ([Campbell and Bozorgnia 2008](#); [Bozorgnia et al. 2010](#)). It uses the same functional form as these peak response relationships, but despite its duration component, the analysis of residuals and statistical metrics shown later in the paper indicate that this functional form is sufficient. However, it is possible that other functional forms could provide an even better fit to the data. Lacking any compelling evidence to the contrary, we prefer to use the same functional form for CAV as we used previously for peak response parameters.

DATABASE

The database used in this study is the same subset of the PEER-NGA strong motion database ([Chiou et al. 2008](#)) that we used to develop our NGA-West empirical GMPEs ([Campbell and Bozorgnia 2007, 2008](#)). It consists of 1,561 recordings from 64 earthquakes with moment magnitudes ranging from 4.3 to 7.9 and rupture distances ranging from 0.1 to 199 km (Figure 2). Details regarding the database are available in [Campbell and Bozorgnia \(2007, 2008\)](#). A complete list of the selected earthquakes and recording stations is provided in Appendix A of [Campbell and Bozorgnia \(2007\)](#).

The ground motion component used to define CAV in this study is the geometric mean of the two as-recorded horizontal components, hereafter referred to as CAV_{GM} . Therefore, CAV_{GM} is undefined if any one of the horizontal components is missing. This definition of the horizontal geometric mean is different from the GMRotI50 horizontal component used in the NGA-West Project (Boore et al. 2006), which is an orientation-independent version of the geometric mean.

GROUND MOTION PREDICTION EQUATION

MEDIAN MODEL

Our CAV_{GM} GMPE uses the functional forms from the NGA-West Project (Campbell and Bozorgnia 2007, 2008). The median GMPE is given by the following general equation:

$$\overline{\ln CAV_{GM}} = f_{mag} + f_{dis} + f_{flt} + f_{hng} + f_{site} + f_{sed} \quad (3)$$

where the magnitude term is given by the expression,

$$f_{mag} = \begin{cases} c_0 + c_1 \mathbf{M}; & \mathbf{M} \leq 5.5 \\ c_0 + c_1 \mathbf{M} + c_2 (\mathbf{M} - 5.5); & 5.5 < \mathbf{M} \leq 6.5 \\ c_0 + c_1 \mathbf{M} + c_2 (\mathbf{M} - 5.5) + c_3 (\mathbf{M} - 6.5); & \mathbf{M} > 6.5 \end{cases} \quad (4)$$

the distance term is given by the expression,

$$f_{dis} = (c_4 + c_5 \mathbf{M}) \ln(\sqrt{R_{RUP}^2 + c_6^2}) \quad (5)$$

the style-of-faulting (fault mechanism) term is given by the expressions,

$$f_{flt} = c_7 F_{RWF_{flt,Z}} + c_8 F_{NM} \quad (6)$$

$$f_{flt,Z} = \begin{cases} Z_{TOR}; & Z_{TOR} < 1 \\ 1; & Z_{TOR} \geq 1 \end{cases} \quad (7)$$

the hanging-wall term is given by the expressions,

$$f_{hng} = c_9 f_{hng,R} f_{hng,M} f_{hng,Z} f_{hng,\delta} \quad (8)$$

$$f_{hng,R} = \begin{cases} 1; & R_{JB} = 0 \\ [\max(R_{RUP}, \sqrt{R_{JB}^2 + 1}) - R_{JB}] / \max(R_{RUP}, \sqrt{R_{JB}^2 + 1}); & R_{JB} > 0, Z_{TOR} < 1 \\ (R_{RUP} - R_{JB}) / R_{RUP}; & R_{JB} > 0, Z_{TOR} \geq 1 \end{cases} \quad (9)$$

$$f_{hng,M} = \begin{cases} 0; & \mathbf{M} \leq 6.0 \\ 2(\mathbf{M} - 6.0); & 6.0 < \mathbf{M} < 6.5 \\ 1; & \mathbf{M} \geq 6.5 \end{cases} \quad (10)$$

$$f_{hng,Z} = \begin{cases} 0; & Z_{TOR} \geq 20 \\ (20 - Z_{TOR})/20; & 0 \leq Z_{TOR} < 20 \end{cases} \quad (11)$$

$$f_{hng,\delta} = \begin{cases} 1; & |\delta| \leq 70 \\ [90 - |\delta|]/20; & |\delta| > 70 \end{cases} \quad (12)$$

the shallow site response term is given by the expression,

$$f_{site} = \begin{cases} c_{10} \ln\left(\frac{V_{S30}}{k_1}\right) + k_2 \left\{ \ln\left[A_{1100} + c\left(\frac{V_{S30}}{k_1}\right)^n\right] - \ln[A_{1100} + c] \right\}; & V_{S30} < k_1 \\ (c_{10} + k_2 n) \ln\left(\frac{V_{S30}}{k_1}\right); & k_1 \leq V_{S30} < 1100 \\ (c_{10} + k_2 n) \ln\left(\frac{1100}{k_1}\right); & V_{S30} \geq 1100 \end{cases} \quad (13)$$

and the basin response (sediment depth) term is given by the expression

$$f_{sed} = \begin{cases} c_{11}(Z_{2.5} - 1); & Z_{2.5} < 1 \\ 0; & 1 \leq Z_{2.5} \leq 3 \\ c_{12}k_3 e^{-0.75[1 - e^{-0.25(Z_{2.5}-3)}]}; & Z_{2.5} > 3 \end{cases} \quad (14)$$

In the above equations, $\ln CAV_{GM}$ is the predicted median value of CAV_{GM} (g-sec); M is moment magnitude; R_{RUP} is the closest distance to the coseismic rupture plane (km); R_{JB} is the closest distance to the surface projection of the coseismic rupture plane (km); F_{RV} is an indicator variable representing reverse and reverse-oblique faulting ($F_{RV}=1$ for $30^\circ < \lambda < 150^\circ$, $F_{RV}=0$ otherwise, and λ is rake angle defined as the average angle of slip measured in the plane of rupture between the strike direction and the slip vector); F_{NM} is an indicator variable representing normal and normal-oblique faulting ($F_{NM}=1$ for $-150^\circ < \lambda < -30^\circ$ and $F_{NM}=0$ otherwise); Z_{TOR} is the depth to the top of the coseismic rupture plane (km); $|\delta| \leq 90^\circ$ is the absolute value of the angle of dip of the rupture plane measured from horizontal; V_{S30} is the time-averaged shear-wave velocity in the top 30 m of the site (m/sec); A_{1100} is the median estimate of the geometric mean horizontal component of PGA on a rock outcrop with $V_{S30}=1100$ m/sec (g); and $Z_{2.5}$ is the depth to the 2.5 km/sec shear-wave velocity horizon, typically referred to as basin or sediment depth (km). We investigated using the value of CAV_{GM} on rock instead of A_{1100} as the ground motion parameter in the nonlinear site response term, but found that the statistical metrics of the regression analysis were not improved. The empirical coefficients were determined using the random-effects regression algorithms of [Abrahamson and Youngs \(1992\)](#), assuming constant variance as justified by [Campbell and Bozorgnia \(2008\)](#). The coefficients are listed in Table 1. This table also lists the coefficients of the PGA relationship of [Campbell and Bozorgnia \(2008\)](#), which can be used to estimate A_{1100} .

We were able to empirically fit the coefficients k_1 and k_2 that were theoretically con-

Table 1. Coefficients for the median and aleatory uncertainty models of CAV_{GM} and PGA

| Coeff. | CAV_{GM} | PGA | Coeff. | CAV_{GM} | PGA | Coeff. | CAV_{GM} | PGA |
|--------|------------|--------|----------|-------------------|---------------------|-------------------|------------|-------|
| c_0 | -4.354 | -1.715 | c_9 | 0.362 | 0.490 | $\sigma_{\ln AF}$ | 0.300 | 0.300 |
| c_1 | 0.942 | 0.500 | c_{10} | 2.549 | 1.058 | $\sigma_{\ln Y}$ | 0.371 | 0.478 |
| c_2 | -0.178 | -0.530 | c_{11} | 0.090 | 0.040 | $\tau_{\ln Y}$ | 0.196 | 0.219 |
| c_3 | -0.346 | -0.262 | c_{12} | 1.277 | 0.610 | σ_C | 0.089 | 0.166 |
| c_4 | -1.309 | -2.118 | k_1 | 400 ^a | 865 ^b | σ_T | 0.420 | 0.526 |
| c_5 | 0.087 | 0.170 | k_2 | -2.690 | -1.186 ^b | σ_{Arb} | 0.429 | 0.551 |
| c_6 | 7.24 | 5.60 | k_3 | 1.0 ^c | 1.839 ^b | ρ | 0.735 | 1.000 |
| c_7 | 0.111 | 0.280 | c | 1.88 ^b | 1.88 ^b | — | — | — |
| c_8 | -0.108 | -0.120 | n | 1.18 ^b | 1.18 ^b | — | — | — |

Note: PGA has units of g, CAV_{GM} has units of g-sec, and standard deviations are in natural log units. Coefficients for PGA are from [Campbell and Bozorgnia \(2008\)](#).

^a k_1 was constrained to 400 because its statistically derived value of 397 was statistically indistinguishable from the smallest theoretical value adopted by [Campbell and Bozorgnia \(2008\)](#).

^b These coefficients were theoretically constrained in the regression ([Campbell and Bozorgnia, 2008](#)).

^c k_3 was arbitrarily set to 1.0 because no theoretical constraint was available. It was included as a parameter to be consistent with the original GMPE of [Campbell and Bozorgnia \(2008\)](#).

strained in the NGA-West GMPE. A hypothesis test determined that the theoretical value for k_1 of 400 used for PGV and PSA ($T \geq 1$ sec) in our previous study was not significantly different at the 99% confidence level from the empirically derived value of 397 in this study. Therefore, we adopted the theoretical value for k_1 , noting that there is no proven theoretical basis for it, and performed a second regression analysis to determine the remaining empirical coefficients. The value of the theoretical coefficient k_3 from the original NGA-West GMPE has no theoretical basis in the current study and was arbitrarily set to 1.0. The coefficients n and c in Equation 13 could not be empirically determined due to their statistical instability. As a result, their theoretical values were adopted from the original NGA-West GMPE. All of the empirical regression coefficients were found to be significant at the 90% confidence level based on their asymptotic standard errors. An R^2 value of 0.94 indicates that a relatively large proportion of the variability in the data is accounted for by the model.

ALEATORY UNCERTAINTY MODEL

The aleatory uncertainty model for CAV_{GM} is defined by the following random-effects equation ([Campbell and Bozorgnia 2008](#)):

$$\ln(CAV_{GM})_{ij} = \overline{\ln(CAV_{GM})_{ij}} + \eta_i + \varepsilon_{ij} \quad (15)$$

where η_i is the interevent residual for event i and where $\overline{\ln(CAV_{GM})_{ij}}$, $\ln(CAV_{GM})_{ij}$, and ε_{ij} are the predicted median value, observed value, and intra-event residual for recording j of event i . The independent normally distributed variables η_i and ε_{ij} have zero means and estimated interevent, intra-event, and total standard deviations (τ , σ , and σ_T , respectively) given by the equations:

$$\tau = \tau_{\ln CAV_{GM}} \quad (16)$$

$$\sigma = \sqrt{\sigma_{\ln(CAV_{GM})_B}^2 + \sigma_{\ln AF}^2 + \alpha^2 \sigma_{\ln(PGA)_B}^2 + 2\alpha\rho\sigma_{\ln(CAV_{GM})_B}\sigma_{\ln(PGA)_B}} \quad (17)$$

$$\sigma_T = \sqrt{\sigma^2 + \tau^2} \quad (18)$$

where $\tau_{\ln CAV_{GM}}$ is the standard deviation of the interevent residuals; $\sigma_{\ln(CAV_{GM})_B} = (\sigma_{\ln CAV_{GM}}^2 - \sigma_{\ln AF}^2)^{1/2}$ is the estimated intraevent standard deviation of $\ln CAV_{GM}$ at the base of the site profile; $\sigma_{\ln CAV_{GM}}$ is the standard deviation of the intra-event residuals; $\sigma_{\ln AF} \approx 0.3$ is the estimated standard deviation of the site amplification factor $\ln AF = f_{site}$ assuming linear site response; $\sigma_{\ln(PGA)_B} = (\sigma_{\ln PGA}^2 - \sigma_{\ln AF}^2)^{1/2}$ is the estimated intra-event standard deviation of $\ln PGA$ at the base of the site profile; $\sigma_{\ln PGA}$ is the estimated intraevent standard deviation of $\ln PGA$; ρ is the correlation coefficient between the intra-event residuals of $\ln CAV_{GM}$ and $\ln PGA$; and α is the linearized functional relationship between f_{site} and $\ln A_{1100}$, which is estimated from the partial derivative $\partial f_{site} / \partial \ln A_{1100}$ according to the expression:

$$\alpha = \begin{cases} k_2 A_{1100} \{ [A_{1100} + c(V_{S30}/k_1)^n]^{-1} - (A_{1100} + c)^{-1} \} & V_{S30} < k_1 \\ 0 & V_{S30} \geq k_1 \end{cases} \quad (19)$$

The value for $\sigma_{\ln AF}$ was assumed to be the same as that used by [Campbell and Bozorgnia \(2008\)](#) for peak response parameters because of its nearly constant value of approximately 0.3 over a relatively large period range ([Bazzurro and Cornell, 2004](#)). We recognize that these results might not extend to an intensity measure that incorporates duration and will address this in a future study.

For some applications, engineers need an estimate of the aleatory uncertainty of the arbitrary horizontal component of ground motion ([Baker and Cornell 2006](#)). The standard deviation of this component can be calculated from the equation:

$$\sigma_{Arb} = \sqrt{\sigma_T^2 + \sigma_C^2} \quad (20)$$

where σ_C is the intracomponent standard deviation of the two horizontal components of ground motion given by the expression ([Boore 2005](#)):

$$\sigma_C^2 = \frac{1}{4N} \sum_{j=1}^N (\ln y_{1j} - \ln y_{2j})^2 \quad (21)$$

in which y_{ij} is the value of the ground motion parameter for component i of recording j and N is the total number of recordings. The coefficients and standard deviations for ground motions subject to linear site response (i.e., for $V_{S30} \geq k_1$ or small values of A_{1100}) in Equations 16–21, along with those for PGA (needed to estimate A_{1100} and $\sigma_{\ln PGA}$) from [Campbell and Bozorgnia \(2008\)](#), are listed in Table 1. A Kolmogorov-Smirnov test indicated that the hypothesis that the interevent, intra-event, and total residuals are normally distributed could not be rejected at the 10% significance level.

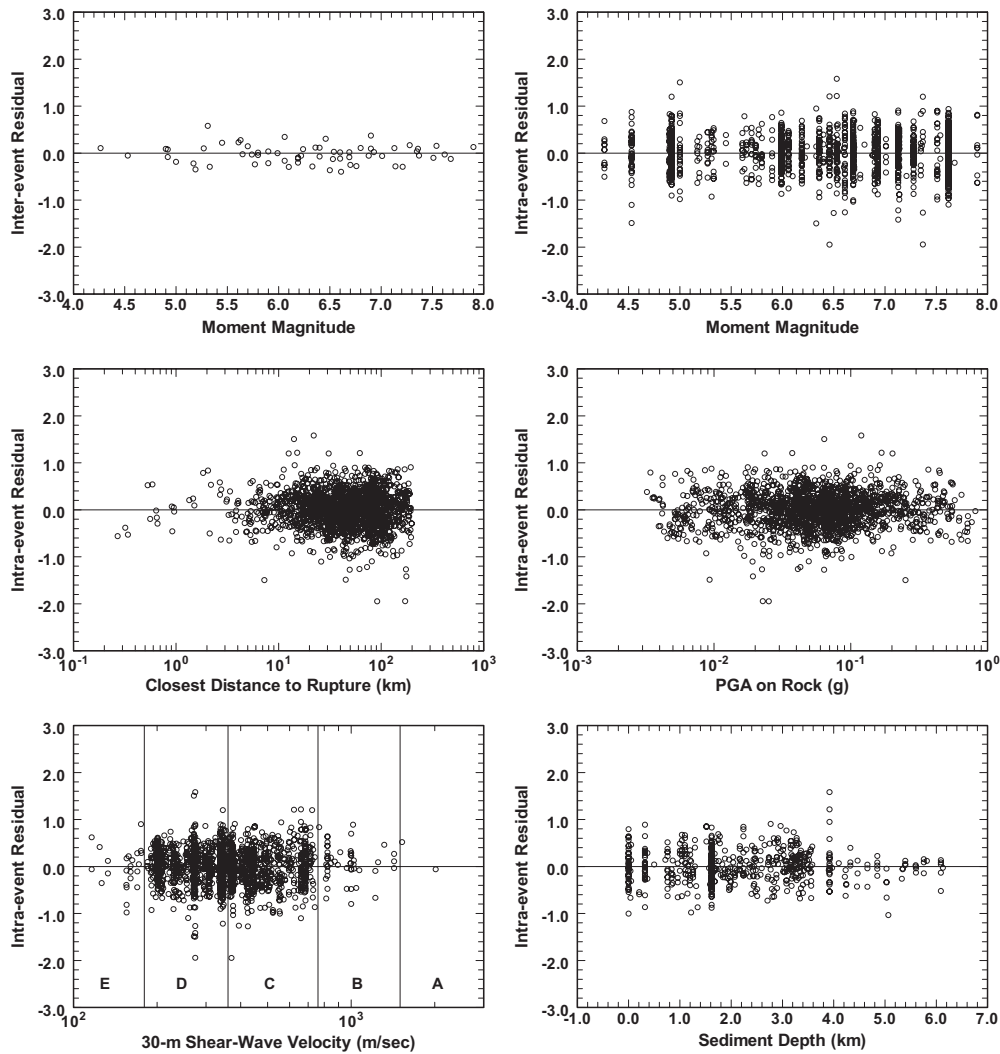


Figure 3. Distributions of interevent and intra-event residuals with respect to moment magnitude (M) and intra-event residuals with respect to rupture distance (R_{RUP}), median PGA on rock (A_{1100}), 30-m shear wave velocity (V_{S30}) binned by NEHRP Site Class, and sediment depth ($Z_{2.5}$).

MODEL VERIFICATION AND EVALUATION

Figure 3 shows the distributions of the interevent and intra-event residuals of $\ln CAV_{GM}$ with respect to M , R_{RUP} , V_{S30} , A_{1100} , and $Z_{2.5}$. These plots confirm that there are no significant biases or trends between the residuals and those predictor variables that were included in the regression analysis. Similar results (not shown) were found for δ , λ , Z_{TOP} , and f_{hmg} . Figure 4 shows how the median estimates of CAV_{GM} scale with respect to R_{RUP} , M , fault mechanism (F_{RV} and F_{NM} for both footwall and hanging-wall sites), NEHRP Site Class,

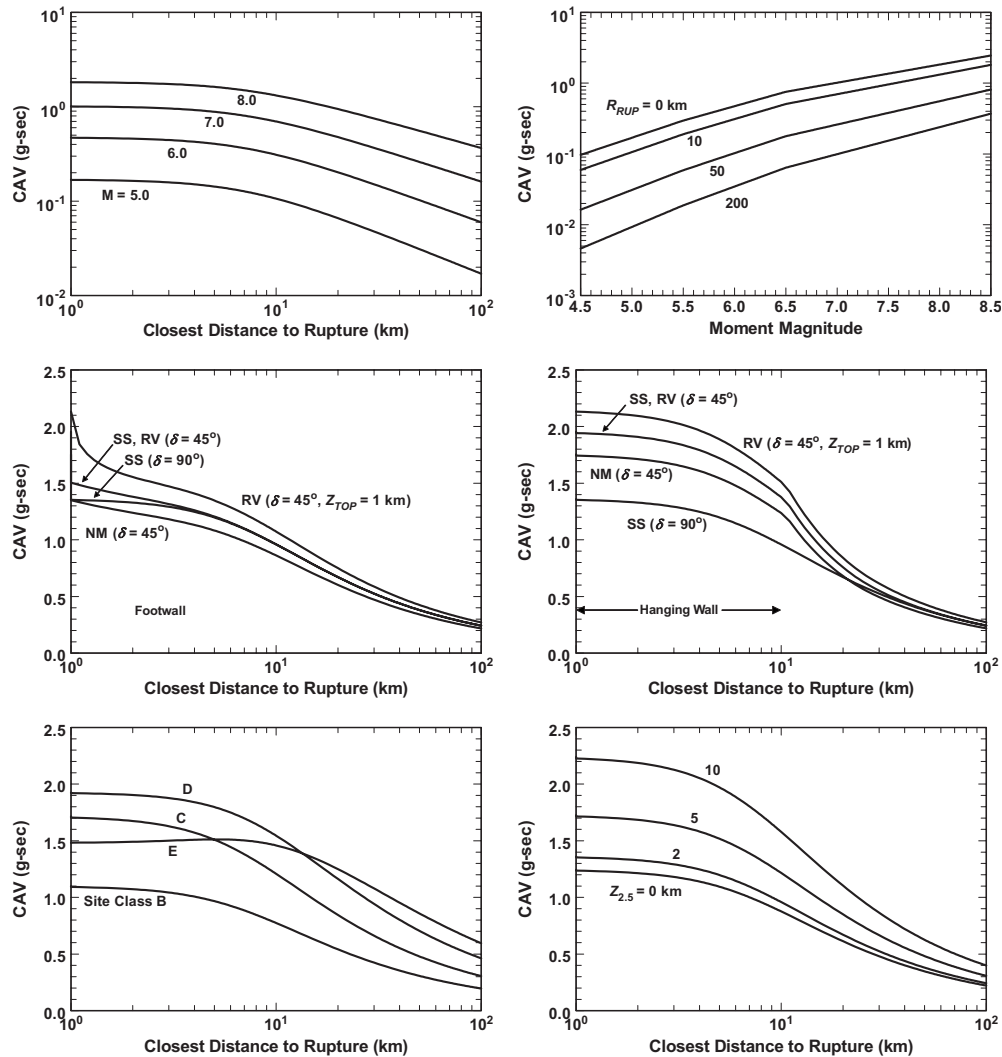


Figure 4. Median predicted values of CAV_{GM} with respect to rupture distance (R_{RUP}), moment magnitude (M), fault mechanism for footwall sites (SS, strike slip; RV, reverse; NM, normal), fault mechanism for hanging-wall sites, NEHRP Site Class, and sediment depth ($Z_{2.5}$). Unless otherwise noted, CAV_{GM} is evaluated for $M=7.5$, vertical strike-slip faulting ($\delta=90^\circ$), surface faulting ($Z_{TOP}=0$), NEHRP Site Class BC ($V_{S30}=760$ m/sec), and $Z_{2.5}=2$ km.

and $Z_{2.5}$. In these plots, NEHRP Site Classes B, C, D, and E are evaluated for 30-m shear-wave velocities of $V_{S30}=1070, 525, 255,$ and 150 m/sec, respectively, which corresponds to the median estimate (logarithmic average) of V_{S30} for each site class (BSSC 2004).

Figure 5 demonstrates the dependence of the predicted site amplification on A_{1100} and $Z_{2.5}$. The plots with respect to A_{1100} show the affect of soil nonlinearity on the predicted

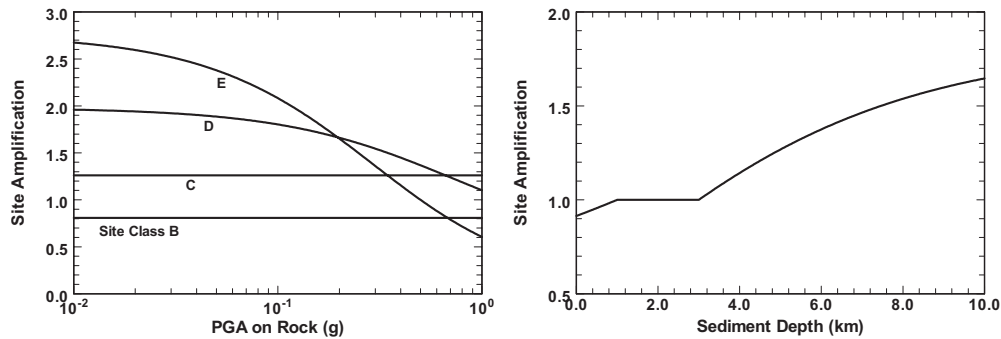


Figure 5. Predicted site effects for CAV_{GM} : (left) amplification factors for NEHRP Site Classes B, C, D, and E (see text for associated values of V_{S30}); (right) amplification factors for sediment depths ($Z_{2.5}$) ranging between 0 and 10 km.

shallow site response for NEHRP Site Classes D and E. Figure 6 shows the dependence of the intra-event and total standard deviations on A_{1100} , which shows the affect of soil nonlinearity on the variability of CAV_{GM} for NEHRP Site Classes D and E.

DISCUSSION

We are only aware of one published GMPE based on the original definition of CAV that we can use to compare with ours (Danciu and Tselentis 2007, hereafter referred to as DT07). This GMPE was developed using the Greek recordings of the European strong motion database. A direct comparison of this relationship with ours is problematic, since it uses epicentral distance as the distance metric, whereas, ours uses closest distance to the coseismic rupture plane. To reduce the impact of these two distance measures, we plot each GMPE against R_{JB} assuming a vertical strike-slip fault. DT07 derived a pseudo

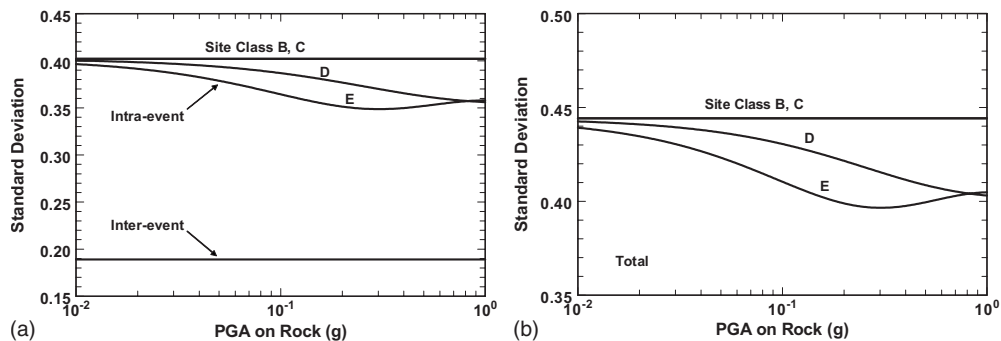


Figure 6. Standard deviations (natural log units) for CAV_{GM} showing their dependence on non-linear site response for NEHRP Site Classes B, C, D, and E (see text for associated values of V_{S30}): (a) interevent and intra-event standard deviations; (b) total standard deviations.

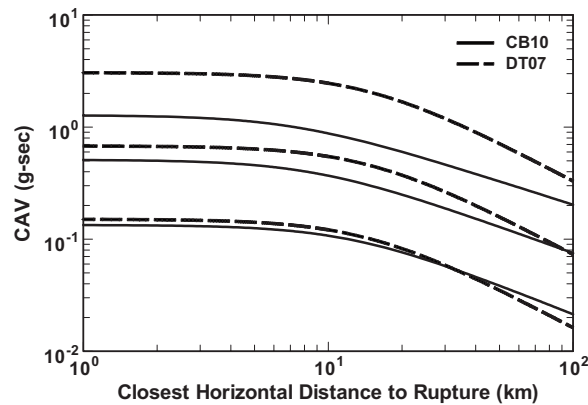


Figure 7. Comparison of the GMPE for CAV_{GM} developed in this study [CB10] with that for CAV developed by [Danciu and Tselentis \(2007\)](#) from shallow crustal earthquakes in Greece [DT07] for $M=5, 6,$ and 7 (bottom to top). See the text for a discussion of how the relationships were evaluated.

depth of 14 km from their regression analysis that approximately accounts for source depth and finite faulting effects. We used a variable depth-to-top of rupture (Z_{TOR}) of 10 km for M 5.0, 5 km for M 6.0, and 0 for M 7.0 in our relationship to approximately account for the expected depth distribution of shallow crustal earthquakes. DT07 defined three site categories to account for local site effects. We evaluated their GMPE for their site category C ($V_{S30}=360-665$ m/sec) and our relationship for NEHRP Site Class C ($V_{S30}=525$ m/sec) and $Z_{2.5}=2$ km.

The two relationships are compared in Figure 7. This plot shows that there is relatively good agreement between the two relationships at small magnitudes, but a lack of magnitude saturation causes DT07 to predict much higher amplitudes close in to large magnitude earthquakes, where data are lacking in the Greek database. The values of τ , σ , and σ_T reported by DT07 (after converting to natural logs) are 0.24, 0.58, and 0.63, respectively. These values are 22%, 56%, and 50% higher than our standard deviations.

One of the more significant results of this study is the statistical robustness of CAV_{GM} , which is better than any of the peak response parameters that we have evaluated thus far ([Campbell and Bozorgnia 2008](#); [Bozorgnia et al. 2010](#)). DT07 found a similar result. Prior to this study, the smallest standard deviations that we had found were for PGA, PGV, and PSA ($T \leq 0.02$ sec). Table 1 shows that there is a reduction of 11% in the interevent standard deviation, 22% in the intra-event standard deviation, 20% in the total standard deviation, 46% in the intracomponent standard deviation, and 22% in the arbitrary horizontal component standard deviation of $\ln CAV_{GM}$ as compared to \ln PGA. The largest reduction is found for the intracomponent standard deviation. In the terminology of performance-based seismic hazard, these results indicate that CAV_{GM} has a higher level of predictability than traditional peak response parameters ([Shome and Cornell 1999](#)).

Several studies have confirmed that the NGA-West GMPEs are generally consistent with strong motion data from shallow crustal earthquakes in active tectonic regions throughout the world. These regions include Europe and the Mediterranean region (Campbell and Bozorgnia 2006; Stafford et al. 2008; Peruš and Fajfar 2010), Taiwan (Lin 2007), Italy (Scasserra et al. 2009), and Iran (Shoja-Taheri et al. 2010). Unpublished results from similar ongoing studies are finding similar results for shallow crustal earthquakes in western Canada, New Zealand, Japan, and Latin America. Therefore, we suggest that the GMPE for CAV_{GM} developed in this study can be used in active tectonic regions worldwide. However, in order to estimate CAV_{GM} in another type of tectonic region, either a new GMPE will need to be developed for this region or the relationship developed in this study will need to be modified to better represent its attenuation characteristics. This could be done using the same hybrid-empirical, stochastic simulation, and numerical modeling methods that have been used to develop GMPEs for eastern North America (see Petersen et al. 2008 for a list of these relationships).

Arias Intensity (AI), defined as the integral of the square of the acceleration time series, has been used more often than CAV as an intensity measure by engineers. However, Danciu and Tselentis (2007) developed GMPEs for both \ln AI and \ln CAV and found that the standard deviation was almost twice as high for \ln AI. A preliminary regression analysis of \ln AI using our database produced the same finding, even though the R^2 value of 0.92 indicated a good fit to the data. Kramer and Mitchell (2006) found a 50% increase in the standard deviation of \ln AI compared to \ln CAV_5 . These results suggest that CAV has significantly higher predictability than AI and should be considered as an alternative to AI in future engineering applications.

CONCLUSIONS

Like the NGA-West relationships that precede them, the GMPE for CAV_{GM} presented in this paper represents a significant advancement in the empirical prediction of ground motion for use in engineering and seismology. It incorporates such important features as non-linear magnitude scaling, magnitude-dependent attenuation, style of faulting, depth of rupture, hanging-wall effects, shallow linear and nonlinear site response, basin response, and amplitude-dependent (nonlinear) intra-event aleatory uncertainty.

We consider the relationships developed in this study to be appropriate for shallow crustal continental earthquakes in active tectonic regions throughout the world. They are most reliable when the predictor variables are limited to the following values: (1) $M > 5.0$, (2) $M < 8.5$ for strike-slip faulting, $M < 8.0$ for reverse faulting, and $M < 7.5$ for normal faulting; (3) $R_{RUP} < 100$ km for $M < 7.0$ and $R_{RUP} < 200$ km for larger magnitudes; (4) $V_{S30} = 150 - 1500$ m/sec or, alternatively, NEHRP Site Classes B ($V_{S30} = 1070$ m/s), C ($V_{S30} = 525$ m/s), D ($V_{S30} = 255$ m/s) and E ($V_{S30} = 150$ m/s); (5) $Z_{2.5} < 10$ km; (6) $Z_{TOR} < 15$ km; and (7) $|\delta| = 15 - 90^\circ$. The recommended upper magnitude limits represent an extrapolation of approximately 0.5 from the largest magnitude of each type of fault mechanism in our database. We believe that this extrapolation is justified given the relationship's strong empirical scaling constraints and unbiased interevent residuals at large magnitudes. We also have extended the applicable range of some of the other predictor variables

beyond the limits of the data when we believe that the relationships have been adequately constrained either empirically or theoretically (Campbell and Bozorgnia 2007, 2008).

The aleatory uncertainty associated with CAV_{GM} is significantly smaller than that found for Arias Intensity or any peak response parameter that we have studied thus far. This makes it a good base model from which to develop GMPEs for other CAV intensity measures that have already been used in specific engineering applications, such as CAV_{STD} (EPRI 1991; USNRC 1997) and CAV_5 (Kramer and Mitchell 2006). The development of relationships between CAV_{GM} and these latter two CAV intensity measures will be the topic of a future study).

ACKNOWLEDGMENTS

This project was partially funded by the International Atomic Energy Agency (IAEA) as part of the activities of Seismic Working Group 1 (WG1) of the Extra Budgetary Program (EBP). Dr. Bozorgnia's participation was partially sponsored by the Pacific Earthquake Engineering Research Center (PEER). Any opinions, findings, and conclusions or recommendations expressed in this material are those of the authors and do not necessarily reflect those of the sponsors. We would like to thank three anonymous reviewers for providing comments that improved the manuscript.

REFERENCES

- Abrahamson, N. A., and Youngs, R. R., 1992. A stable algorithm for regression analyses using the random effects model, *Bull. Seismol. Soc. Am.* **82**, 505–510.
- Arias, A., 1970. A measure of earthquake intensity, in *Seismic Design for Nuclear Power Plants*, R. J. Hansen (ed.), The MIT Press, Cambridge, MA, 438–483.
- Baker, J. W., and Cornell, C. A., 2006. Which spectral acceleration are you using?, *Earthquake Spectra* **22**, 293–312.
- Bazzarro, P., and Cornell, C. A., 2004. Nonlinear soil-site effects in probabilistic seismic-hazard analysis, *Bull. Seismol. Soc. Am.* **94**, 2110–2123.
- Boore, D. M., 2005. Erratum: equations for estimating horizontal response spectra and peak acceleration from western North American earthquakes: a summary of recent work, *Seismol. Res. Lett.* **76**, 368–369.
- Boore, D. M., Watson-Lamprey, J., and Abrahamson, N., 2006. Orientation-independent measures of ground motion, *Bull. Seismol. Soc. Am.* **96**, 1502–1511.
- Bozorgnia, Y., Hachem, M. M., and Campbell, K. W., 2010. Ground motion prediction equation (“attenuation relationship”) for inelastic response spectra, *Earthquake Spectra*, **26**, 1–23.
- Building Seismic Safety Council (BSSC), 2004. *NEHRP Recommended Provisions for Seismic Regulations for New Buildings and Other Structures (FEMA 450)*, 2003 edition, National Institute of Building Sciences, Washington, D. C.
- Cabañas, L., Benito, B., and Herráiz, M., 1997. An approach to the measurement of the potential structural damage of earthquake ground motions, *Earthquake Eng. Struct. Dyn.* **26**, 79–92.
- Campbell, K. W., and Bozorgnia, Y., 2006. Next generation attenuation (NGA) empirical ground motion models: can they be used in Europe?, in *Proc., First European Conference on*

- Earthquake Engineering and Seismology*, Paper No. 458, Geneva, Switzerland, 10 pp.
- , and Bozorgnia, Y., 2007. *Campbell-Bozorgnia NGA Ground Motion Relations for the Geometric Mean Horizontal Component of Peak and Spectral Ground Motion Parameters*, PEER Report No. 2007/02, Pacific Earthquake Engineering Research Center, University of California, Berkeley, 238 pp.
- , and Bozorgnia, Y., 2008. NGA ground motion model for the geometric mean horizontal component of PGA, PGV, PGD and 5% damped linear elastic response spectra for periods ranging from 0.01 to 10 s, *Earthquake Spectra* **24**, 139–171.
- , and Bozorgnia, Y., 2010. *Analysis of Cumulative Absolute Velocity (CAV) and JMA Instrumental Seismic Intensity (I_{JMA}) Using the PEER-NGA Strong Motion Database*, PEER Report No. 2010/01, Pacific Earthquake Engineering Research Center, University of California, Berkeley, 83 pp.
- Chiou, B., Darragh, R., Gregor, N., and Silva, W., 2008. NGA project strong-motion database, *Earthquake Spectra* **24**, 23–44.
- Danciu, L., and Tselentis, G., 2007. Engineering ground-motion parameters attenuation relationships for Greece, *Bull. Seismol. Soc. Am.* **97**, 162–183.
- Electrical Power Research Institute (EPRI), 1988. *A Criterion for Determining Exceedance of the Operating Basis Earthquake*, Report No. EPRI NP-5930, Palo Alto, California.
- , (EPRI), 1991. *Standardization of the Cumulative Absolute Velocity*, Report No. EPRI TR-100082-T2, Palo Alto, California.
- , (EPRI), 2006. *Program on Technology Innovation: Use of Cumulative Absolute Velocity (CAV) in Determining Effects of Small Magnitude Earthquakes on Seismic Hazard Analyses*, Report No. 1014099, Palo Alto, California.
- Housner, G. W., 1959. Behavior of structures during earthquakes, *J. Eng. Mech. Div. ASCE* **85**, 104–129.
- Klügel, J. U., Mualchin, L., and Panza, G. G., 2006. A scenario-based procedure for seismic risk analysis, *Eng. Geol.* **88**, 1–22.
- Koliopoulos, P. K., Margaris, B. N., and Klimis, N. S., 1998. Duration and energy characteristics of Greek strong motion records, *J. Earthquake Eng.* **2**, 390–417.
- Kostov, M., 2005. Site specific estimation of Cumulative Absolute Velocity, in *Proc., 18th International Conference on Structural Mechanics in Reactor Technology (SMiRT 18)*, Beijing, China, 3041–3050.
- Kramer, S. L., and Mitchell, R. A., 2006. Ground motion intensity measures for liquefaction hazard evaluation, *Earthquake Spectra* **22**, 413–438.
- Lin, P. S., 2007. *A Comparison Study of Earthquake Strong-Ground Motions in California and in Taiwan*, PEER Report No. 2006/12, Pacific Earthquake Engineering Research Center, University of California, Berkeley.
- Martinez-Rueda, J. E., Moutsokapas, G., and Tsantali, E., 2008. Predictive equations to estimate Arias Intensity and Cumulative Absolute Velocity as a function of Housner Intensity, in *Proc., Seismic Engineering Conference Commemorating the 1908 Messina and Reggio Calabria Earthquake*, Messina, Italy, 309–306.
- Peruš, I., and Fajfar, P., 2010. Ground-motion prediction by a non-parametric approach, *Earthquake Eng. Struct. Dyn.*, in press.
- Petersen, M., Frankel, A., Harmsen, S., Mueller, C., Haller, K., Wheeler, R., Wesson, R., Zeng, Y., Boyd, O., Perkins, D., Luco, N., Field, E., Wills, C., and Rukstales, K., 2008. *Documen-*

- tation for the 2008 Update of the United States National Seismic Hazard Maps, U. S. Geol. Survey Open-File Report 2008-1128.
- Power, M., Chiou, B., Abrahamson, N., Bozorgnia, Y., Shantz, T., and Roblee, C., 2008. An overview of the NGA project, *Earthquake Spectra* **24**, 3–21.
- Scasserra, G., Stewart, J. P., Bazzurro, P., Lanzo, G., and Mollaioli, F., 2009. Comparison of NGA ground motion prediction equations to Italian data, *Bull. Seismol. Soc. Am.* **99**, 2961–2978.
- Shoja-Taheri, J., Naserieh, S., and Ghofrani, H., 2010. A test of the applicability of NGA models to the strong ground motion data in the Iranian Plateau, *J. Earthquake Eng.* **14**, 278–292.
- Shome, N., and Cornell, C. A., 1999, *Probabilistic Seismic Demand Analysis of Nonlinear Structures*, Report No. RMS-35, *Reliability of Marine Structures Program*, Department of Civil and Environmental Engineering, Stanford University, Stanford, California.
- Stafford, P. J., 2008. Conditional prediction of absolute durations, *Bull. Seismol. Soc. Am.* **98**, 1588–1594.
- Stafford, P. J., Strasser, F. O., and Bommer, J. J., 2008. An evaluation of the applicability of the NGA models to ground-motion prediction in the Euro-Mediterranean region, *Bulletin Earthquake Engineering* **6**, 149–177.
- Tselentis, G., and Danciu, L., 2008. Empirical relationships between Modified Mercalli Intensity and engineering ground motion parameters in Greece, *Bull. Seismol. Soc. Am.* **98**, 1863–1875.
- U. S. Nuclear Regulatory Commission (USNRC), 1997. *Pre-Earthquake Planning and Immediate Nuclear Power Plant Operator Postearthquake Actions*, Regulatory Guide 1.166, Washington, D. C., 8 pp.
- Watson-Lamprey, J. A., and Abrahamson, N. A., 2007. Use of minimum CAV in seismic hazard analyses, in *Proc., 9th Canadian Conference on Earthquake Engineering*, Ottawa, 352–358.

(Received 9 October 2009; accepted 12 January 2010)